Available online at www.sciencedirect.com

SCIENCE DIRECT®

ELSEVIER

Nuclear Instruments and Methods in Physics Research A 524 (2004) 124–129

NUCLEAR INSTRUMENTS & METHODS IN PHYSICS RESEARCH Section A

www.elsevier.com/locate/nima

# Recent advances in X-ray detection with micro-hole and strip plate detector

J.F.C.A. Veloso[a,b,*], J.M. Maia[c,1], L.F. Requicha Ferreira[a,d], J.M.F. dos Santos[a], A. Breskin[c], R. Chechik[c], Rui de Oliveira[e]

[a] *Physics Department, University of Coimbra, P-3004-516 Coimbra, Portugal*
[b] *Physics Department, University of Aveiro, P-3810-193 Aveiro, Portugal*
[c] *Department of Particle Physics, The Weizmann Institute of Science, 76100 Rehovot, Israel*
[d] *Physics Department, University of Beira Interior, P-6201-001 Covilhã, Portugal*
[e] *CERN 1211 Geneve 23 EST/DEM/PMT, Switzerland*

Received 5 January 2004; accepted 7 January 2004

**Abstract**

We report on the performance of a micro-hole and strip plate, fabricated with standard gas electron multiplier-production procedures, presenting 40-μm hole-diameter and 30-μm wide anode strips. Multiplication factors of $5 \times 10^4$ were reached in an Ar/Xe (95/5) atmosphere at about 1 bar; the energy resolution is of the order of 14% (FWHM) for 5.9-keV X-rays.


*PACS:* 29.40.−n; 29.40.Cs; 85.60.Gz

*Keywords:* Microstrip gas counter; Gas electron multiplier; Micro-hole & strip plate

## 1. Introduction

The introduction of the gas electron multiplier (GEM) [1] prompted a new generation of radiation gas detectors with a wide range of applications. The GEM is an array of sub-millimetre holes, etched through a thin polymer substrate, with conductors deposited on each side. The avalanche process occurs within the holes under the intense electric field established by a suitable potential difference between the two surface electrodes. Gains exceeding $10^3$ are achieved with a single GEM; higher gains can be obtained by cascading several GEMs or by coupling GEMs with other gaseous electron multipliers. It was demonstrated that a micro-strip gas counter (MSGC) [2] preceded by a GEM has higher gain and stability compared to the MSGC alone [3]. Localization can be obtained in GEM detectors by coupling a properly patterned readout anode to a GEM [4]. Very high multiplication factors, exceeding $10^6$–$10^7$, have been measured with single photoelectrons in gas-avalanche photomultipliers combining a photocathode and cascaded GEM structures [5].

*Corresponding author. Physics Department, University of Coimbra, P-3004-516 Coimbra, Portugal. Tel.: +351-239-410-667; fax: +351-239-829-158.

*E-mail address:* jveloso@gian.fis.uc.pt (J.F.C.A. Veloso).

[1] On leave from University of Coimbra and University of Beira Interior, Portugal.

0168-9002/$ - see front matter 
doi:10.1016/j.nima.2004.01.057

The lack of photon-feedback permitted high-gain operation also in noble-gas mixtures, including Ar–Xe [5].

The micro-hole and strip plate (MHSP) [6–9] is a new micro-patterned structure, shown in Fig. 1. It combines the features of both GEM and MSGC in a single double-sided micro-structure: a continuous top-electrode and an MSGC-like structured bottom face. It provides two successive independent charge-amplification stages: electrons are preamplified within the GEM-like holes and the resulting avalanche electrons are further multiplied on the bottom strips. The holes are aligned within the cathode strips, while the anode strips run between them. The special shape of the anode-strip ends and the cathode electrode shape around them was designed to prevent discharges. Similarly to the GEM, an electric field is established within the holes through a potential difference, $V_{hole}$, between the top-electrode and the cathode strips; the potential difference, $V_{ac}$, between the anode and cathode strips, establishes an MSGC-like electric field on the bottom part of the MHSP. With this design, the voltages between the top-electrode and the cathodes, and between the cathodes and the anodes, can be maintained well below their breakdown threshold, while achieving total gas gains similar, or even higher, than those obtained with a single GEM or MSGC [9]. An important additional advantage of this design is the significant reduction of photon feedback and avalanche-ion back-flow, discussed in detail in Refs. [10–12]. The multiplication properties of MHSPs and of cascaded multi-GEM and MHSP have been systematically investigated in Refs. [9,12].

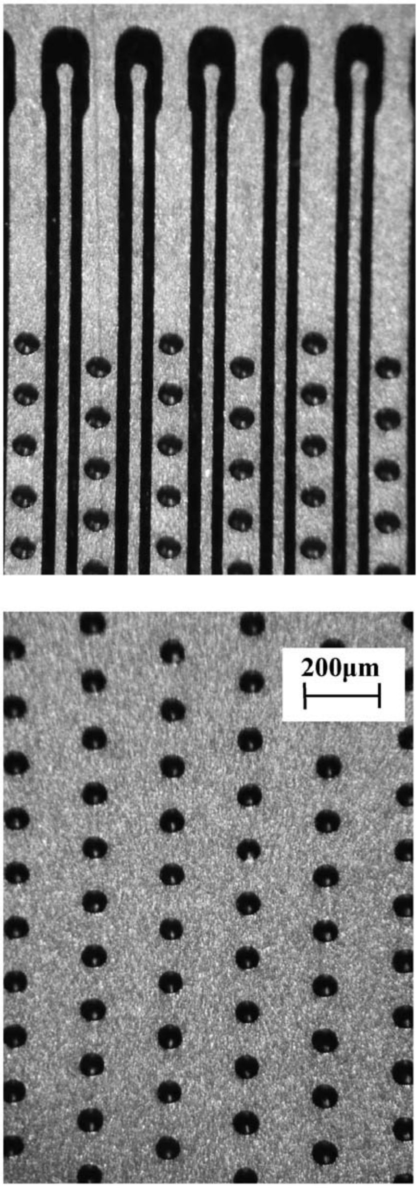


Fig. 1. Photomicrographs of the MHSP used in this work: (a) top-side and (b) micro-strip bottom-side.

Similarly to GEMs, the MHSP can be fabricated using flexible printed circuit board (PCB) technology. However, the MHSP characteristics are still limited by their manufacturing imperfections, resulting in a low production yield. In the present work, we report on the performance of an MHSP, chosen for its better quality, investigated with soft X-rays, in atmospheric Ar–5% Xe gas mixture. In particular, we discuss detector gain, energy resolution and minimum detectable X-ray energy.

## 2. Experimental set-up and description

A schematic view of the MHSP principle of operation is depicted in Fig. 2. The MHSP active area is $2.8 \times 2.8\,cm^2$. The kapton and the copper film-thicknesses are 50 and 5 μm, respectively. The

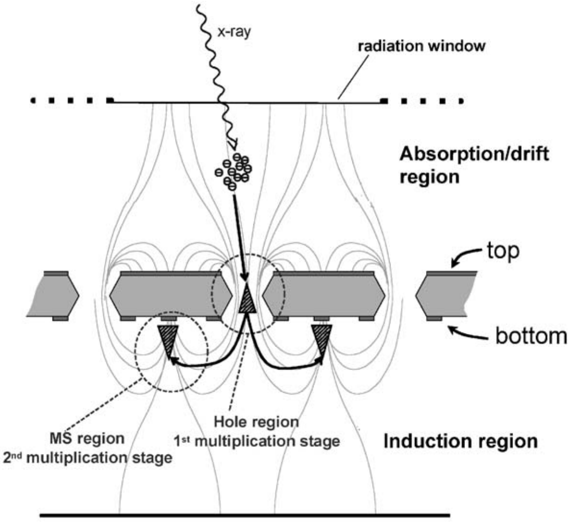


Fig. 2. Schematic of the MHSP-based detector.

micro-strip anode and cathode widths are 30 and 100 μm, respectively, with a 200-μm pitch. The anode–cathode gap is 35 μm. The MHSP holes are bi-conical, of diameters 40 μm in the kapton and 70 μm in the copper film; they are arranged in an asymmetric hexagonal lattice of 140- and 200-μm pitch in the directions parallel and perpendicular to the strips, respectively. The MHSP, enclosed between two stainless-steel meshes, is assembled in a stainless-steel vessel. The absorption/drift region and the charge induction region are 3-mm wide.

Most soft X-rays interact in the absorption/drift region above the MHSP, and the resulting primary electron cloud drifts along the field lines towards the MHSP holes. The electrons undergo charge multiplication in the holes; the avalanche-electrons emerge on the other side of the MHSP, where they are directed towards the anode strips and further multiplied in the high anode-strips field. For these events, double-stage multiplication occurs. A small fraction of X-rays may be absorbed in the induction region below the MHSP, depositing electron clouds that experience charge multiplication only at the anode strips, and resulting in much smaller amplitude pulses. The gain of the MHSP holes can be derived from the relative peak positions of the two event types. The detector was filled with an Ar–5% Xe mixture at 1.07 bar, continuously purified through getters [SAES St172/HI/7–6/150C] at 150°C, and maintained in circulation by convection. This gas mixture is known to be a Penning mixture, providing high gain at relatively low voltages [5,8]; it is simple to purify and has no ageing problems.

All electrodes were independently polarized. The electrode of the induction region was grounded; the drift electrode mesh was operated at negative voltage, to ensure insensitivity to X-ray interactions above the mesh. The cathode strips voltage was kept constant throughout this work, at 30 V (induction field of ~100 V/cm). The electric field in the drift region was kept constant at ~50 V/cm. In order avoid damaging of the MHSP; the bias voltages used in this study were always kept below the micro-discharge onset.

Detector signals were fed through a Canberra 2006 preamplifier (sensitivity of 1.5 V/pC) and a Tennelec TC243 linear-amplifier (4-μs shaping time, 8-μs peaking time) to an EG&G 8096-multichannel analyser. The electronic chain sensitivity was calibrated for absolute gain determination, using a calibrated capacitor directly connected to the preamplifier input and to a precision pulse generator.

We used 5.9-keV X-rays from a $^{55}$Fe source, filtered through a chromium film to remove the 6.4-keV Mn-$K_\beta$ X-rays; for gain calibrations we have also employed 22.1-keV Ag-$K_\alpha$ X-rays from a $^{109}$Cd source, as discussed below. For peak-amplitude and energy resolution determination, pulse-height distributions were fitted to a Gaussian superimposed on a linear background.

## 3. Experimental results and discussion

Fig. 3 presents the total gain of the MHSP and the energy resolution as a function of $V_{ac}$, maintaining $V_{hole}$ at 260 V. The experimental data reveal a characteristic exponential development of the charge avalanche process in the proportional regime. Total gains as high as $5\times10^4$ were reached, about an order of magnitude higher than those typically achieved with GEMs in Ar-hydrocarbon gas mixtures [4,5,13]. The rather large width of the present anode strips limits their

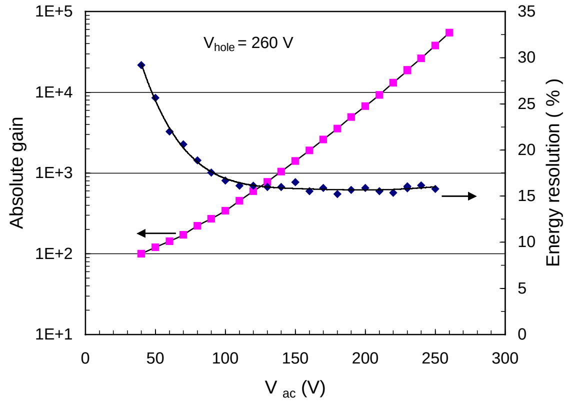


Fig. 3. MHSP total gain and detector energy resolution (5.9-keV X-rays) as a function of $V_{ac}$, for $V_{hole} = 260\,V$, and for Ar–5% Xe, 1 atm.

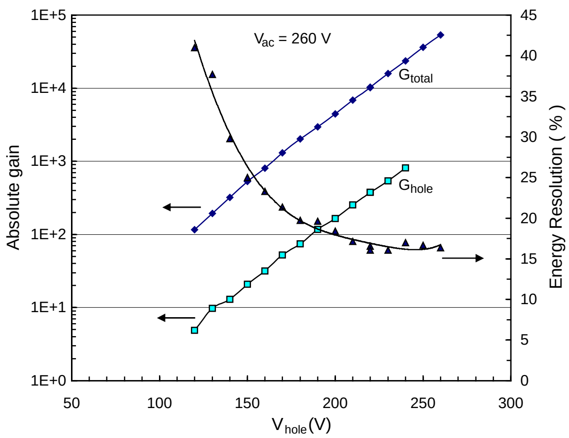


Fig. 4. MHSP total gain, holes gain and detector energy resolution (5.9-keV X-rays) as a function of $V_{hole}$, for $V_{ac} = 260\,V$, and for Ar–5% Xe, 1 atm.

electric field strength; consequently, the maximum achievable gain in this second amplification stage is limited to about 30. In principle, higher gains should be attainable with thinner strips, as demonstrated in Ref. [9]. The energy resolution shown in Fig. 3 converges to a minimum value of 16% FWHM for $V_{ac}$ values above 130 V; this is a significant improvement compared to the 23% FWHM energy resolution recorded with MHSPs of the previous generation [9].

Fig. 4 depicts the MHSP's total gain, the holes gain and the energy resolution, as a function of

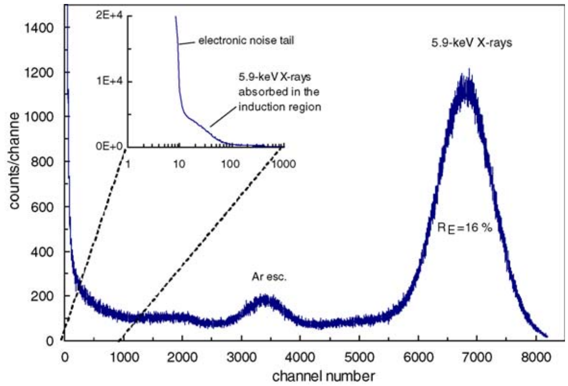


Fig. 5. Typical pulse-height distribution for 5.9-keV X-rays and $V_{ac} = V_{hole} = 260\,V$, for Ar–5% Xe at 1 atm, acquired during 50 h.

$V_{hole}$, maintaining $V_{ac}$ at 260 V. The highest gains recorded in the MHSP holes, of about $10^3$, are similar to those obtained with GEMs. The energy resolution improves with increasing $V_{hole}$, converging to the minimum value of 16% for $V_{hole}$ above 220 V.

A typical pulse-height distribution obtained with this detector for 5.9-keV X-rays is presented in Fig. 5, for $V_{hole} = V_{ac} = 260\,V$. The salient spectral features include the full-energy absorption-peak from X-ray interactions in the absorption/drift region, the Ar K-fluorescence escape-peak, the electronic-noise tail in the low-energy end and a broad distribution under the electronic-noise tail, which results from X-ray interactions in the induction region. As shown in Fig. 5, the low-energy limit due to the electronic-noise tail is of the order of 10 channels. This demonstrates the good prospects for the application of this micro-structure to very soft X-ray detection. Moreover, taking into account that the mean energy to produce an electron–ion pair in argon–xenon mixtures is about 22 eV, the use of the MHSP for single-electron detection seems to be a realistic possibility. Since the 5.9 keV X-ray interactions on the induction region are not completely separated from the electronic noise, due to the low anode-strips gain, the gain of the MHSP holes was obtained from pulse-height spectra of 22.1-keV Ag-$K_\alpha$ X-rays (emitted from a $^{109}$Cd X-ray radioactive source), by comparing

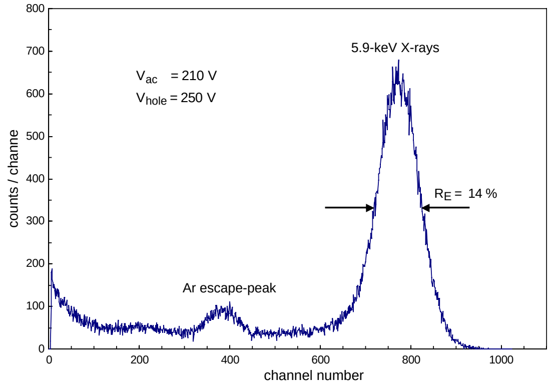


Fig. 6. Typical pulse-height distribution for 5.9-keV X-rays, for best energy resolution conditions $V_{ac} = 210\,V$ and $V_{hole} = 250\,V$, and for Ar–5% Xe at 1 atm.

peak-heights from absorptions in the absorption/drift region and in the induction region.

It is possible to further improve the detector's energy resolution, by better tuning the different electrodes biasing. For example, energy resolutions of about 14% FWHM was reached with $V_{ac} = 210\,V$ and $V_{hole} = 250\,V$, as shown in Fig. 6. Moreover, the detector can be made less sensitive to X-ray interactions in the induction region, by reducing its width and better tuning its electric field [8]. Note that the pulse-height distribution presented in Fig. 5 was acquired throughout 50 h and does not show significant degradation in the obtained energy resolution or electronic-noise tail, when compared to pulse-height distributions recorded over few minutes, e.g. Fig. 6.

## 4. Summary and discussion

The experimental results obtained with this MHSP confirm a very stable operation, free of spurious pulses and/or micro-discharges, and without significant drift in the detector's pulse amplitude. The present MHSP has 30-μm wide anodes instead of the 10 μm of the previous MHSP generation [9]; the thicker anodes result in lower strip gain, about 30, but in a more stable MHSP operation. It is expected, though, that future MHSPs can be safely produced with 15–20-μm wide anode strips, if required.

Total gains around $5 \times 10^4$ were reached with soft X-rays in a single MHSP structure operated with atmospheric Ar–5% Xe. This gain, which could be in principle further enhanced with thinner anode strips, is about an order of magnitude higher than the typical gain of a single GEM. In the best operation conditions reached in this work, an energy resolution of about 14% FWHM was obtained with 5.9-keV X-rays.

The low-energy limit due to electronic-noise tail is rather low, indicating good prospects for the application of this micro-structure to soft X-rays detection and possibly to that of single-electrons. However, one should keep in mind that one could precede the MHSP with a GEM or with a cascade of GEMs; the latter would permit reaching higher gains and more stable operation, with reduced ion feedback [9,12].

2D charge imaging with the MHSP can be done in different ways. For example, the anode strips can provide one coordinate, while the other one could be obtained by structuring the top MHSP face into strips running orthogonally to the anode ones [6]. With suitable biasing voltages, the signal induced on the top MHSP electrode can have as much as 50% of the anode-strip signal-height [14,15]. An alternative approach is to obtain the second coordinate, or both coordinates, from the positive ions collected on the cathode plane coupled to the MHSP at the induction region; this plane can be structured and placed at close proximity, of several hundred microns, from the MHSP [15].

The fact that the MHSP operates in a stable way in Ar/Xe is of a prime importance. We presently investigate Gas Proportional Scintillation Counters (GPSC) for X-ray spectroscopy and imaging, where the scintillation light is detected in the same gas volume with MHSP-based gas photomultipliers with CsI photocathodes. The latter can be reflective ones, deposited on the top face of the MHSP or on that of a preceding GEM, as shown in Ref. [16].

## Acknowledgements

Support is acknowledged to Fundação para a Ciência e a Tecnologia (FCT), Lisbon (under

POCTI and FEDER programs), through project POCTI/FNU/49553/02 of the Instrumentation Centre (unit 217/94), Physics Department, University of Coimbra, by the Israel Science Foundation and by the Planning and Budgeting Committee of the Council for Higher Education in Israel. J.F.C.A. Veloso and J.M. Maia acknowledge support grants from FCT. A. Breskin is the Reuther Professor of Research in Peaceful use of Atomic Energy.

## References

[1] F. Sauli, Nucl. Instr. and Meth. A 386 (1997) 531.
[2] A. Oed, Nucl. Instr. and Meth. A 263 (1988) 351.
[3] R. Bouclier, W. Dominik, M. Hoch, J.C. Labbe, G. Million, L. Ropelewski, F. Sauli, A. Sharma, G. Manzini, Nucl. Instr. and Meth. A 396 (1997) 50.
[4] A. Bressan, R. De Oliveira, A. Gandi, J.-C. Labbe, L. Ropelewski, F. Sauli, D. Mörmann, T. Muller, H.J. Simonis, Nucl. Instr. and Meth. A 425 (1999) 254.
[5] A. Buzulutskov, A. Breskin, G. Garty, R. Chechik, F. Sauli, L. Shekhtman, Nucl. Instr. and Meth. A 443 (2000) 164.
[6] J.F.C.A. Veloso, J.M.F. dos Santos, C.A.N. Conde, Rev. Sci. Instrum. 71 (2000) 2371.
[7] J.F.C.A. Veloso, J.M. Maia, R.E. Morgado, J.M.F. dos Santos, C.A.N. Conde, Rev. Sci. Instrum. 73 (2002) 488.
[8] J.M. Maia, J.F.C.A. Veloso, R.E. Morgado, J.M.F. dos Santos, C.A.N. Conde, IEEE Trans. Nucl. Sci. 49 (2002) 875.
[9] J.M. Maia, J.F.C.A. Veloso, J.M.F. dos Santos, A. Breskin, R. Chechik, D. Mörmann, Nucl. Instr. and Meth. A 504 (2003) 364.
[10] D. Mörmann, M. Balcerzyk, A. Breskin, R. Chechik, B.K. Singh, A. Buzulutskov, Nucl. Instr. Meth. A 504 (2003) 93.
[11] D. Mörmann, A. Breskin, R. Chechik, D. Bloch, Nucl. Instr. and Meth. A 516 (2004) 315.
[12] J.M. Maia, D. Mörmann, A. Breskin, R. Chechik, J.F.C.A. Veloso, J.M.F. dos Santos, Avalanche-ion backflow reduction in gaseous electron multipliers based on GEM/MHSP, Nucl. Instr. and Meth. A, in press.
[13] J. Benlloch, A. Bressan, M. Capeáns, M. Gruwé, M. Hoch, J.C. Labbé, A. Placci, L. Ropelewski, F. Sauli, Nucl. Instr. and Meth. 419 (1998) 410.
[14] G. Cicognani, D. Feltin, B. Guerard, A. Oed, 1997-IEEE Nuclear Science Symposium, Conference Record, Vols. 1 and 2, 1998, pp. 296–298.
[15] J.M. Maia, D. Mörmann, A. Breskin, R. Chechik, J.F.C.A. Veloso, J.M.F. dos Santos, 2D Localization Properties of GEM/MHSP Radiation Detectors, in preparation.
[16] D. Mörmann, A. Breskin, R. Chechik, P. Cwetanski, B.K. Singh, Nucl. Instr. and Meth. A 478 (2002) 230.